



Contents lists available at ScienceDirect

# Current Research in Pharmacology and Drug Discovery

journal homepage: [www.journals.elsevier.com/current-research-in-pharmacology-and-drug-discovery](http://www.journals.elsevier.com/current-research-in-pharmacology-and-drug-discovery)



## Fabrication and evaluation of mannose decorated curcumin loaded nanostructured lipid carriers for hepatocyte targeting: *In vivo* hepatoprotective activity in Wistar rats



Manish Kumar Gupta<sup>a</sup>, Vipul Sansare<sup>a,c,\*</sup>, Birendra Shrivastava<sup>a</sup>, Santosh Jadhav<sup>b</sup>, Prashant Gurav<sup>c</sup>

<sup>a</sup> School of Pharmaceutical Sciences, Jaipur National University, Jaipur, 302017, India

<sup>b</sup> Department of Pharmaceutical Chemistry, SVPM'S College of Pharmacy, Malegaon, Maharashtra, 413115, India

<sup>c</sup> Department of Pharmaceutics, Indira Institute of Pharmacy, Sadavali, Maharashtra, 415804, India

### ARTICLE INFO

#### Keywords:

D-mannose  
Mannose stearylamine conjugate  
Asialoglycoprotein receptors  
Curcumin  
Hepatocytes targeting

### ABSTRACT

Curcumin is a well-recognized antioxidant phytoactive isolated from the rhizomes of *Curcuma longa*. Numerous landmark investigations have proved the antioxidant and hepatoprotective potential of curcumin. The aim of present study was to target curcumin loaded nanocarriers to hepatocytes using asialoglycoprotein receptors targeting strategy. Mannose, a water-soluble carbohydrate, was hydrophobized by anchoring stearylamine with an objective to conjugate mannose on the surface of curcumin loaded nanostructured lipid carriers for targeting asialoglycoprotein receptors on hepatocytes. Mannose conjugated stearylamine was synthesized and characterized using various analytical techniques. The synthesized targeting ligand was incorporated curcumin loaded nanostructured lipid carriers and characterized by photon correlation spectroscopy. Zeta potential measurement was used to confirm the conjugation of the synthesized ligand to the surface of drug-loaded nanostructured lipid carriers. CCl<sub>4</sub> induced hepatotoxicity in male Wistar rats was used as an experimental animal model to evaluate the hepatoprotective potential of formulated drug encapsulated nanostructured lipid carriers. The hepatoprotective potential was assessed by measuring serum liver injury markers and oxidative stress parameters in the liver post-mitochondrial supernatant. Mannose conjugated nanostructured lipid carriers showed acceptable particle size which revealed its suitability for hepatocyte targeting. In addition to this, mannose conjugated nanocarriers revealed significantly better ( $p < 0.05$ ) reduction of serum liver injury markers and proinflammatory cytokines compared to the unconjugated one which confirmed hepatocytes targeting potential of the synthesized ligand. Asialoglycoprotein receptors targeting could be a landmark strategy for hepatocyte targeting. Thus, the synthesized mannose anchored stearylamine could be a promising novel targeting ligand having hepatocyte targeting potential.

### 1. Introduction

Liver is a complex and specialized organ which regulates numerous biochemical functions like synthesis and metabolism of a number of complex molecules. Various liver diseases affect millions of people worldwide, which are difficult to treat with conventional drug delivery (Bartneck et al., 2014). World Health Organization has reported 30–50% of liver cirrhosis globally due to alcohol consumption and more than 300 million cases of chronic hepatitis infections in 2020 (Vasanthkumar et al., 2017). Numerous drugs have been investigated for the treatment of

diseases associated with liver, however a correct drug delivery system needs to be found for the delivery of drugs.

Majority of conventionally administered drugs are accumulated in the liver, however, the efficient therapeutic effect in diseases like hepatocellular carcinoma, hepatitis, liver cirrhosis and hepatic tuberculosis is not achieved. To overcome the limitations associated with conventional drug delivery, novel colloidal carriers like liposomes (Castangia et al., 2015; Shah et al., 2013; Tang and Ge, 2017), nanoparticles (NPs) (Guhagarkar et al., 2015; Raposo et al., 2020), solid lipid nanoparticles (SLNs) (Bonferoni et al., 2018; Kakkar and Kaur, 2012; Mohanlakshmi

\* Corresponding author. School of Pharmaceutical Sciences, Jaipur National University, Jaipur, 302017, India.

E-mail address: [avipulsansare@gmail.com](mailto:avipulsansare@gmail.com) (V. Sansare).

<https://doi.org/10.1016/j.crphar.2022.100083>

Received 1 October 2021; Received in revised form 1 January 2022; Accepted 10 January 2022

2590-2571/© 2022 The Authors. Published by Elsevier B.V. This is an open access article under the CC BY-NC-ND license (<http://creativecommons.org/licenses/by-nc-nd/4.0/>).

**Table 1**  
Physical characteristics of mannose and NODM.

Characteristics	Mannose	NODM
Colour	White	Pale yellow
Solubility	Aqueous solvent	Organic solvent

et al., 2019; Prathyusha et al., 2014), nanostructured lipid carriers (Nahr et al., 2019) and phytosomes (Permana et al., 2020; Tung et al., 2011) were widely investigated by many formulation scientists. These colloidal carriers offer numerous advantages including ease of surface conjugation with targeting ligands for cell specific delivery (Sansare et al., 2020). Hepatocyte targeting is a challenging concept to the formulation experts because the lack of surface receptor expression on these cells. The carbohydrate receptors expressed on hepatic parenchymal cells are called as asialoglycoprotein receptor (Pranatharthi et al., 2017). These receptors specifically recognize carbohydrates like mannose, galactose, fructose and fucose (Shah et al., 2013). Thus, conjugation of these carbohydrates on the surface of drug-loaded nanocarriers could be a promising strategy for hepatocytes specific delivery of drug. In addition to this, carbohydrates have better potential to bind with receptors expressed on various cell types and can also provide a stealth protection to colloidal carriers like liposome and NPs (Irache et al., 2008; Jain et al., 2012). Numerous researchers have successfully utilized carbohydrates as a targeting ligands for liver targeting of drug encapsulated nanocarriers.

Wu et al., 2009 (Wu, 2009) have attempted to formulate prednisone loaded NPs for liver targeted drug delivery using galactose as a targeting ligand. The *in vivo* studies proved better targeting potential of galactose

modified drug-loaded NPs compared to conventional NPs. The studies also showed better uptake of galactose decorated drug-loaded NPs in liver. This could be due to surface conjugation of NPs with galactose which is responsible for liver-specific delivery of NPs. Guo et al., (2014) (Guo et al., 2014) have utilized galactose as a targeting ligand for hepatocytes targeted delivery of doxorubicin. The fabricated drug-loaded NPs revealed better uptake of drug in liver compared to kidney and heart. Craparo et al., (2014) (Craparo et al., 2014) have successfully proved the use of galactose for liver targeted delivery of sorafenib. The galactose modified sorafenib encapsulated micelles showed specific distribution in mouse liver on oral administration. Bei et al., (2014) (Bei et al., 2014) have formulated lactose conjugated self-assembled micelles for hepatocyte specific delivery of harmine. Formulated drug-loaded micelles exhibited significantly better inhibition of tumor growth in H22 tumor-bearing mice. In addition to this, fluorescence spectroscopy confirmed better liver targeting potential of lactose modified micelles. The major findings of these studies can suggest the use of carbohydrates for efficient liver targeting of drug-loaded nanocarriers.

Carbon tetrachloride ( $\text{CCl}_4$ ) induced hepatic injury is the best suitable animal model of free radical-mediated hepatotoxicity (Rechnagel and EAJ, 1973). Metabolism of  $\text{CCl}_4$  results in the formation of a trichloromethyl free radical,  $\text{CCl}_3^*$ . The resulted free radicals mediates the production of reactive oxygen species through the cytochrome P450 oxygenase system. The reactive oxygen species causes lipid peroxidation and lastly hepatocellular damage.  $\text{CCl}_3^*$  interacts with cellular molecules like nucleic acids, protein and lipid, which eventually leads to lipid metabolism impairment and fatty degeneration i.e., steatosis.

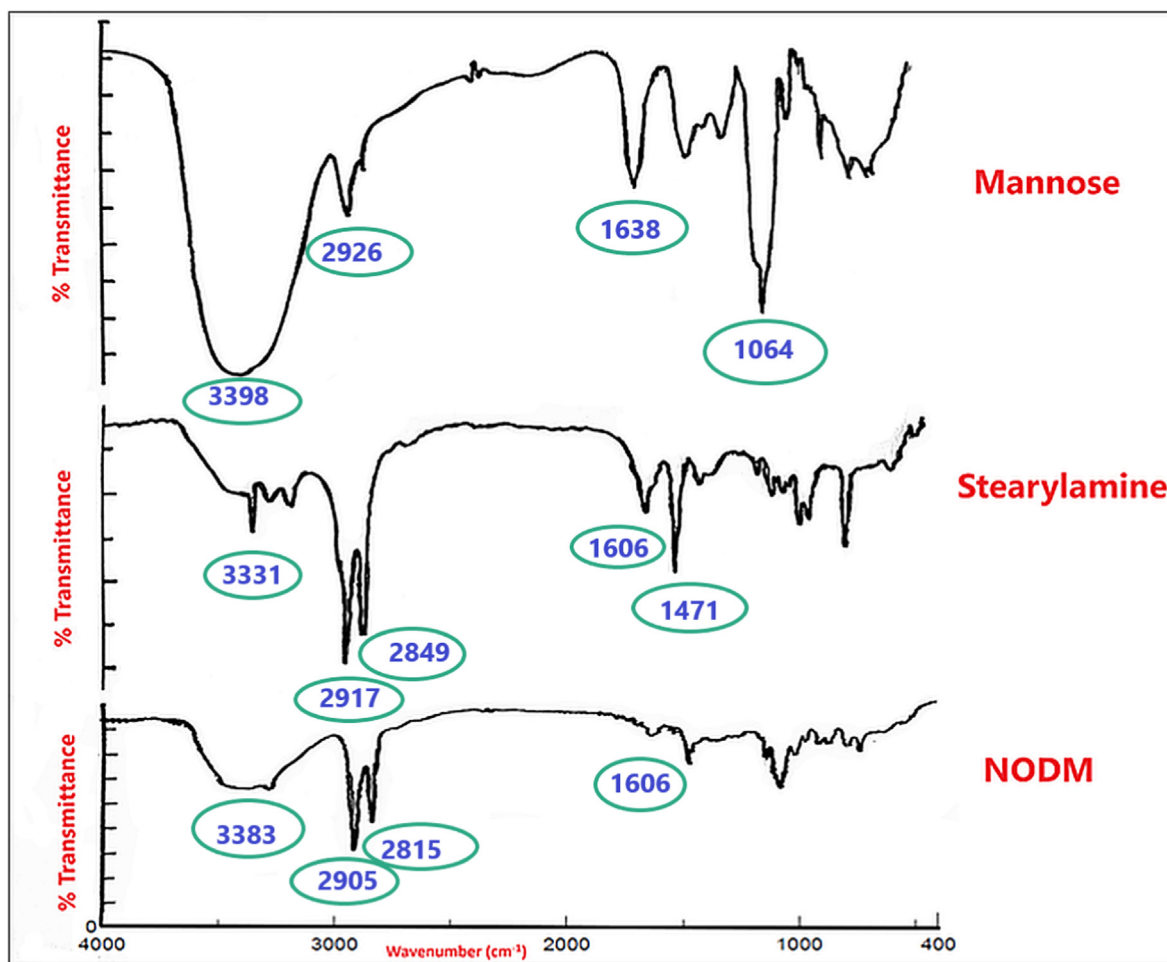


Fig. 1. FTIR spectra of mannose, stearylamine and synthesized NODM.

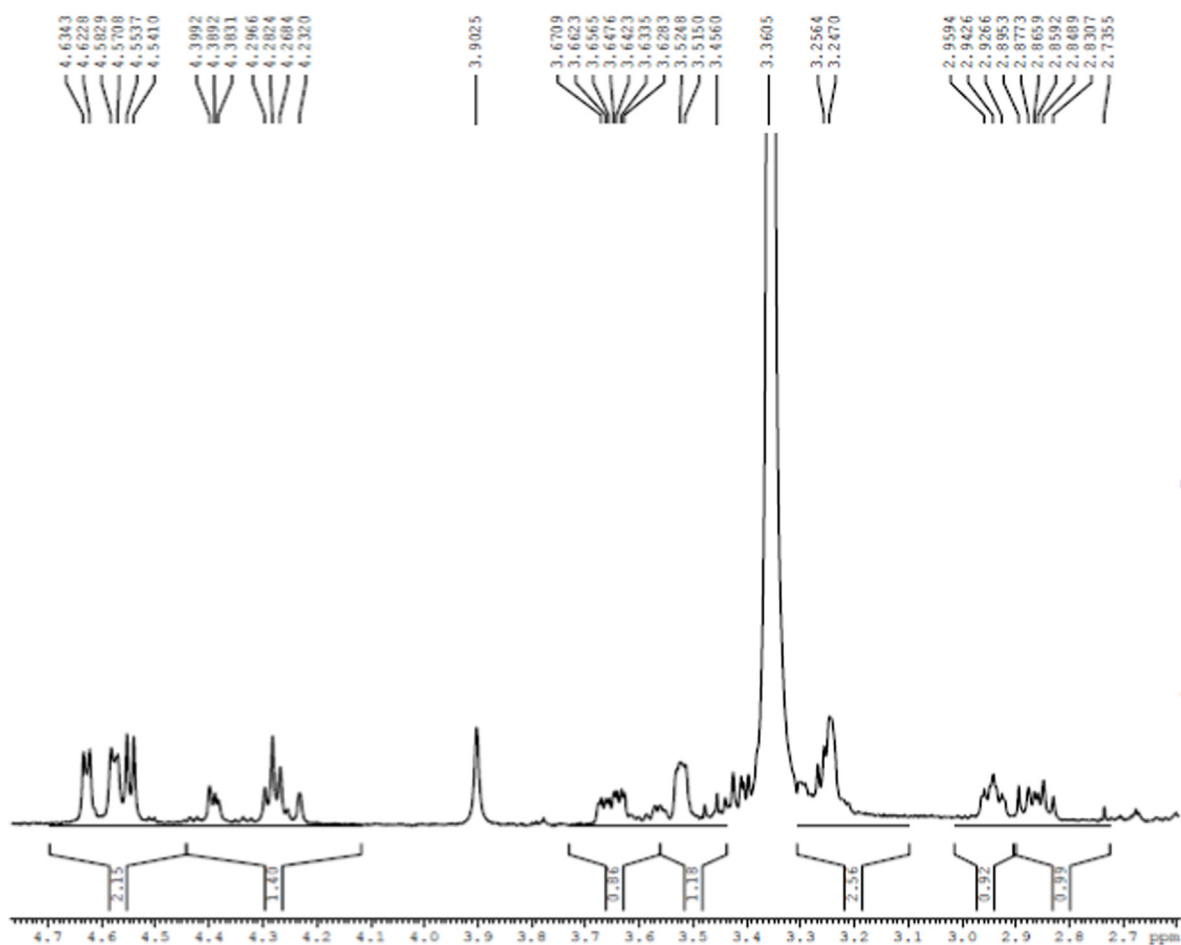


Fig. 2.  $^1\text{H}$  NMR spectra of synthesized NODM.

Curcumin, which is polyphenolic antioxidant phytoactive extracted from rhizomes of *Curcuma longa* (Mimche et al., 2011). Numerous landmark studies have proved the antioxidant and hepatoprotective properties of curcumin in animal models (Farzaei et al., 2018). Curcumin has reported to modulate inflammatory mediator activity and scavenges various reactive oxygen species, which makes it suitable phytoactive for hepatoprotection (Rivera-espinosa and Muriel, 2009).

Thus, aim of the present work was the synthesis and characterization of a mannose conjugated stearylamine with potential to target the asialoglycoprotein receptor of hepatocytes. Mannose and stearylamine was synthesized and characterized by various analytical techniques and incorporated into curcumin loaded NLCs which were evaluated by photon correlation spectroscopy. Hepatoprotective potential of the fabricated curcumin loaded NLCs was assessed using  $\text{CCl}_4$  induced hepatotoxic animal model. The mannose decorated NLCs showed significantly better hepatoprotection compared to unconjugated NLCs.

## 2. Material and methods

### 2.1. Material

Stearylamine, curcumin and D-mannose were purchased from Sigma-Aldrich Co. LLC (USA). Soya lecithin S-100 was obtained as gift sample from Lipoid (Germany). Stearic acid and Dynasan 118® were obtained

from Sasol Germany (Germany). Tween 20 and oleic acid were obtained from S.D. Fine Chemicals Ltd. (India). Geleol®, Compritol 888 ATO and Precirol 5® were obtained from Gattefosse (USA). All other solvents chemicals and reagents were purchased locally.

### 2.2. Synthesis and characterization of *N*-octadecyl-mannopyranosylamine

Mannose anchored stearylamine was synthesized using the method as mentioned by Witoonsaridsilp W et al. (Witoonsaridsilp et al., 2012). Briefly, stearylamine (5 mM) was solubilized in ethanol (15 ml) and heated up to 70 °C using heating mantle, after complete dissolution of stearylamine, the D-mannose (5 mM) was added with stirring (200 rpm). The resulting ethanolic solution was stirred for 15 min for complete dissolution of mannose. At last, solution was cooled to 40 °C and mixed with 35 ml of n-hexane to obtain NODM crystals. The formed NODM crystals were then purified using dialysis technique and dried.

#### 2.2.1. Fourier-transform infrared spectroscopy (FTIR)

Stearylamine, mannose and synthesized targeting ligand NODM were subjected to FTIR spectroscopy (Jasco FTIR-5300, Japan). The KBr disk method was used to prepare samples for FTIR analysis. All samples were mixed with KBr separately and the resulting powder mixture converted into a thin KBr disk by compression in a die at 10 tons pressure. At last, FTIR spectrums of all samples were recorded.

	<b>Size (d.nm):</b>	<b>% Volume:</b>	<b>St Dev (d.nm):</b>
<b>Z-Average (d.nm):</b> 170.4	<b>Peak 1:</b> 204.1	100.0	77.51
<b>Pdl:</b> 0.186	<b>Peak 2:</b> 0.000	0.0	0.000
<b>Intercept:</b> 0.937	<b>Peak 3:</b> 0.000	0.0	0.000
<b>Result quality :</b> <b>Good</b>			

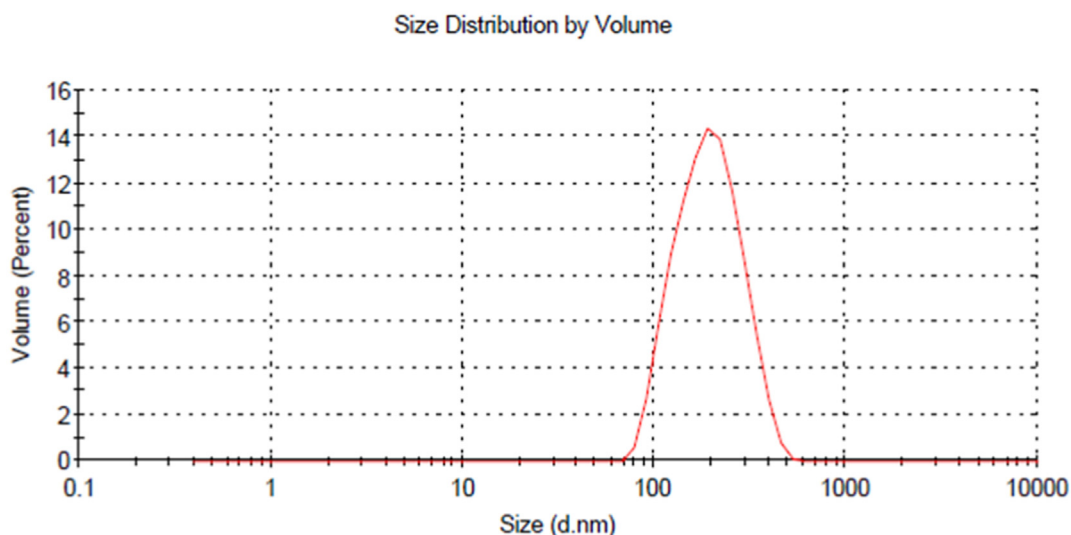


Fig. 3. Intensity plot showing particle size distribution of conventional curcumin NLCs.

	<b>Size (d.nm):</b>	<b>% Volume:</b>	<b>St Dev (d.nm):</b>
<b>Z-Average (d.nm):</b> 181.0	<b>Peak 1:</b> 175.5	100.0	51.45
<b>Pdl:</b> 0.209	<b>Peak 2:</b> 0.000	0.0	0.000
<b>Intercept:</b> 0.983	<b>Peak 3:</b> 0.000	0.0	0.000
<b>Result quality :</b> <b>Refer to quality report</b>			

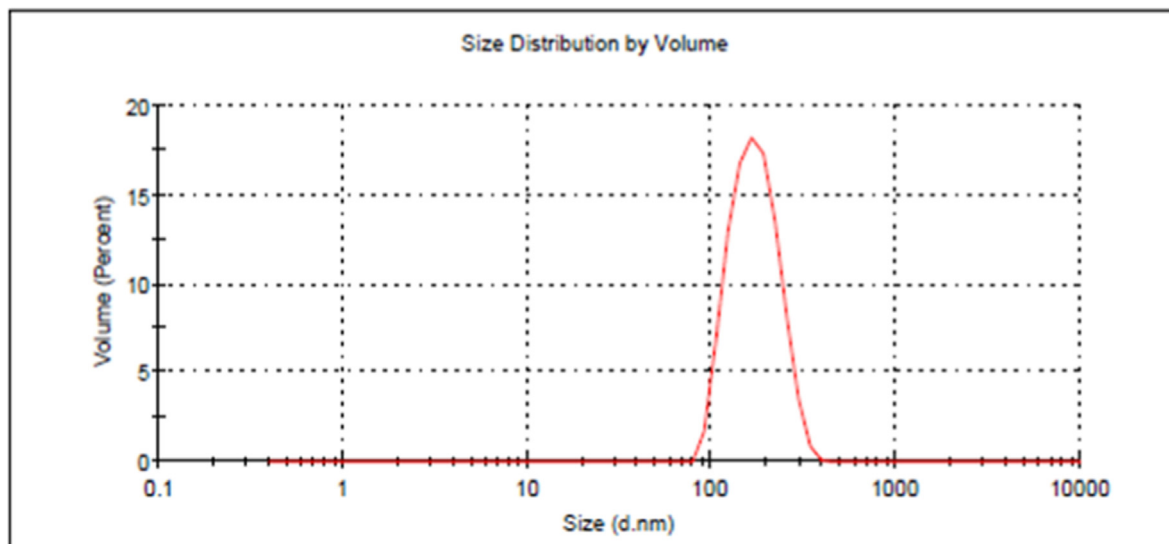


Fig. 4. Intensity plot showing particle size distribution of mannosylated curcumin NLCs.

2.2.2. Proton nuclear magnetic resonance (<sup>1</sup>H NMR)

Proton NMR of synthesized targeting ligand NODM was measured using NMR spectrometer (Bruker Avance II 400) at frequency 400 MHz.

The CDCl<sub>3</sub> was used as deprotonated solvent to dissolve NODM while recording NMR spectrum.

**Table 2**

Zeta potentials of NODM curcumin NLCs (n = 3).

Formulation	Zeta potential (mV)
Conventional curcumin NLCs	-12.19 ± 0.641
NODM curcumin NLCs (1%)	-18.18 ± 0.43
NODM curcumin NLCs (5%)	-27.71 ± 0.537
NODM curcumin NLCs (10%)	-34.19 ± 0.461

**Table 3**% Inhibition in ALT and AST levels in treatment groups with respect to CCl<sub>4</sub> group (n = 6).

Group	% Inhibition of ALT versus CCl <sub>4</sub> group	% Inhibition of AST versus CCl <sub>4</sub> group
Group III	45.75 ± 2.78	73.45 ± 3.51
Group IV	63.17 ± 3.472	81.37 ± 3.162
Group V	52.73 ± 2.913	75.42 ± 3.17

### 2.3. Fabrication and characterization of conventional as well as mannose decorated curcumin loaded NLCs

The melt homogenization coupled with high energy ultrasonication technique was used to fabricate conventional and mannose decorated curcumin encapsulated NLCs. Stearic acid and oleic acid (8:2) mixture was melted at 70 °C to form molten lipid phase. Curcumin with or without NODM (10% w/w of total lipid) were dissolved in molten lipid phase and soya lecithin S-100 was transferred in the resulting melted lipids. An aqueous phase containing surfactant was prepared using 10 ml of distilled water as well as Tween 20 and maintained at 70 °C. The resulting aqueous surfactant phase was injected using syringe (24 gauge) into molten lipid phase and stirred continuously at 4000 rpm for 10 min using overhead stirrer (Remi, India). The obtained hot emulsion was sonicated using probe sonicator (VCX500, Sonics and materials, USA) at 20% amplitude for 10 min and stored. For further particle size reduction, both NLCs were homogenize using high pressure homogenizer (Stansted, UK) at 10,000 psi for 3 cycles.

#### 2.3.1. Particle size distributions

The photon correlation spectroscopy principle (Zetasizer Nano ZS,

Malvern, UK) was successfully utilized for assessment of particle size of fabricated NLCs dispersions. NLCs dispersions were diluted with double distilled water to reduce particle count and better accuracy of results. The resulting diluted dispersions subjected to particle size assessment at 24 °C (Sansare et al., 2019).

#### 2.3.2. Assessment of percent entrapment of curcumin in NLCs matrix

An ultracentrifugation technique was used to assess percent encapsulation of curcumin in lipid matrix of NLCs. Briefly curcumin containing NLC dispersions were ultra-centrifuged at 80,000 rpm for 1 h at 4 °C using ultracentrifuge (Optima Max XP, Beckman Coulter, USA) to form NLCs pellet and separate the free/unencapsulated curcumin. At last, supernatant was removed, diluted and analyzed by UV spectrophotometry at  $\lambda_{\text{max}}$  of 424 nm using methanol AR as a blank for quantification of free drug. Percentage encapsulation of curcumin in lipid matrix of NLCs was calculated by using equation.

$$\text{Percent entrapment efficiency} = \frac{\text{WL} - \text{WF}}{\text{WL}} \times 100$$

where, WL is the quantity of curcumin initially added in the dispersion and WF is the amount of curcumin quantified in supernatant.

#### 2.4. Assessment of in vivo liver protective potential

Male Wistar rats weighing 150 to 200 gm were selected as animals to confirm the liver targeting potential of the targeting ligand NODM. The protocol of animal study was supervised and approved by the Institutional Animals Ethical Committee of Indira Institute of Pharmacy (Approval number: IIP/IAEC/08/2019–20). All animals were obtained from ISO registered source, Global bioresearch solution Pvt. Ltd, Shirwal, India.

Rats were placed in cages and kept on standard diet. Rats were randomly divided into five groups, each having 6 rats. Group I was marked as vehicle control (VC) group and administered standard vehicle i.e. olive oil at the dose of 1 ml/kg BW. Group II served as positive control (PC) and received the standard liver toxic drug CCl<sub>4</sub>. Group III was marked as the standard group and received standard liver protective product i.e. Liv-52 at the dose of 1 ml/kg BW (Mayuren et al., 2010). Group IV animals were treated with mannosylated curcumin NLCs at the dose of 20 mg/kg BW. Group V animals were treated with conventional curcumin NLCs at the dose of 20 mg/kg BW.

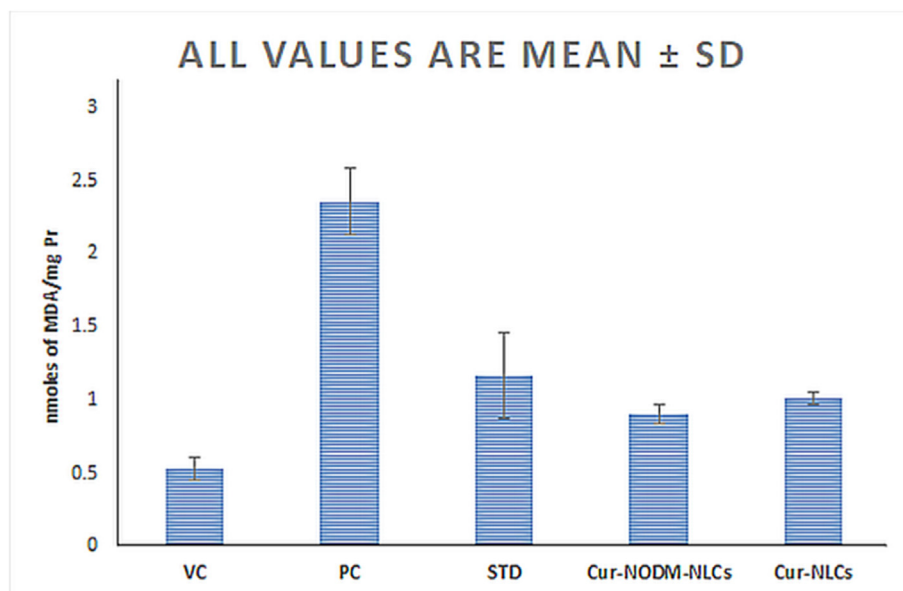


Fig. 5. MDA levels on treatment with curcumin -NLCs, mannosylated curcumin NLCs and different control groups after CCl<sub>4</sub> induced hepatotoxicity.

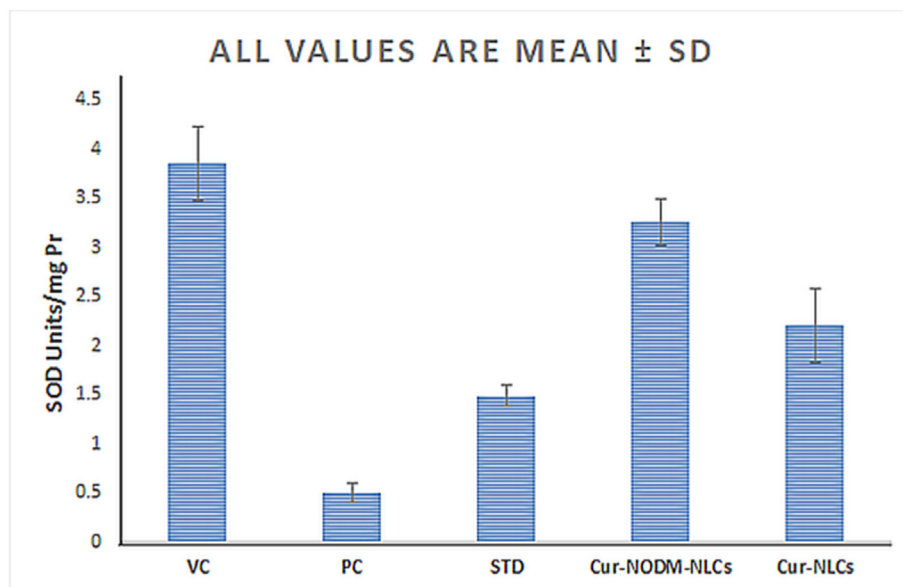


Fig. 6. SOD levels on treatment with curcumin -NLCs, mannosylated curcumin NLCs and different control groups after CCl<sub>4</sub> induced hepatotoxicity.

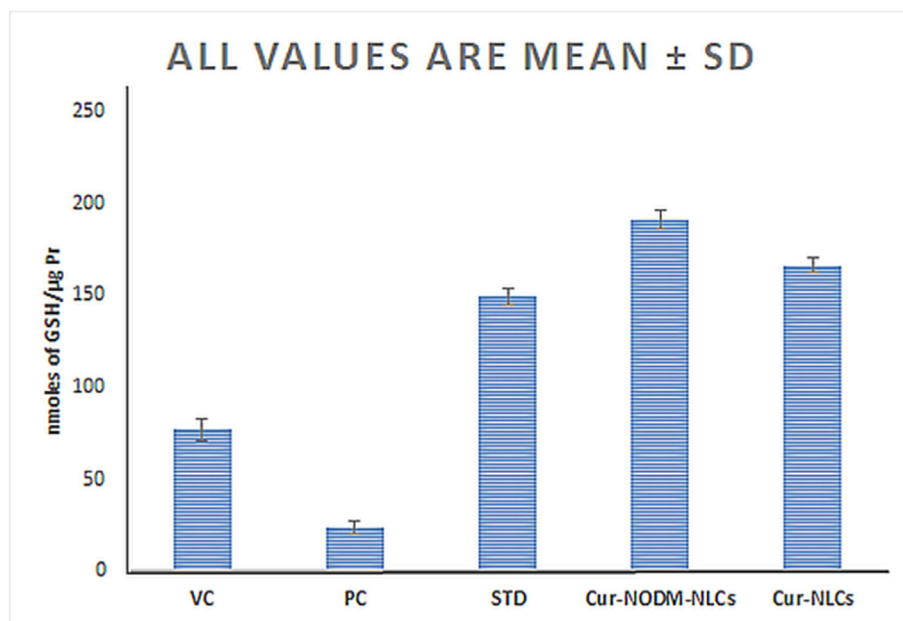


Fig. 7. Chart showing comparative GSH levels on administration of curcumin -NLCs, mannosylated curcumin NLCs and different control groups after CCl<sub>4</sub> induced hepatotoxicity.

CCl<sub>4</sub> (dispersed in an equal volume of olive oil) was administered in 24 rats at the dose of 4 ml/kg BW for 10 days to induce liver tissue injury. In VC group, 1 ml/kg BW of olive oil was administered for 10 days (liver injury was not induced in VC group). In the standard group, three days after the final dose of CCl<sub>4</sub>, Liv-52 was administered at a dose of 1 ml/kg BW daily for four weeks. In group IV, three days after final dose of CCl<sub>4</sub> as in the standard group, mannosylated curcumin NLCs were administered at a dose of 20 mg/kg BW daily for four weeks. In group V, three days after the last dose of CCl<sub>4</sub> as in the standard group, conventional curcumin NLCs were administered at a dose of 20 mg/kg BW daily for four weeks (Singh et al., 2015).

At the end of the treatment schedule, rats were anesthetized using ether and blood was removed through retro-orbital plexus. The removed blood was centrifuged at 4000 rpm for 20 min at 4 °C to separate serum from blood. The isolated serum was used for measurement of liver injury markers. All animals were sacrificed at the end of study protocol and liver

was harvested to estimate oxidative stress parameters. In the PC group, animals were sacrificed three days after the final dose of CCl<sub>4</sub> i.e., on 13th day, and all other animals were sacrificed on the 42nd day, i.e., a day after the final treatment period. After harvesting, the liver was homogenized with 10% (w/v) cold phosphate buffered saline (PBS, pH 7.4). The liver post-mitochondrial supernatant (PMS) was used to assess oxidative stress parameters. PMS was obtained by centrifugation of rat liver homogenates in the phosphate buffer pH 7.4 for 20 min at 4 °C.

#### 2.4.1. Estimation of serum liver injury markers

Estimation of serum liver injury markers such as ALT, AST is essential operation to measure the hepatoprotective efficacy of curcumin NLCs and liver targeting efficiency of the synthesized ligand. The standard diagnostic kits (Reckon diagnostic, India) was used to estimate liver injury markers.

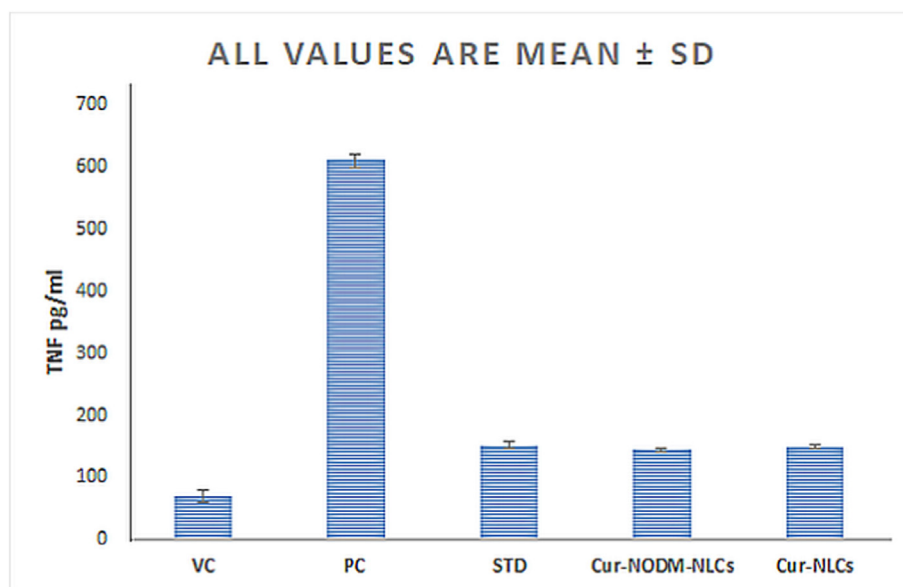


**Fig. 8.** Comparative TNF- $\alpha$  levels on four weeks treatment with curcumin -NLCs, mannosylated curcumin NLCs and different control groups after CCl<sub>4</sub> induced hepatotoxicity.

#### 2.4.2. Estimation of antioxidant parameters

The prepared liver PMS was used to estimate oxidative stress parameters like LPO, SOD, and GSH.

**2.4.2.1. Estimation of LPO.** The LPO level in liver PMS was measured according to technique mentioned in published literature (Wills, 1966). The malondialdehyde (MDA) level, a measure of LPO, was measured as liver thiobarbituric acid species. The LPO levels in experimental animals were denoted as nanomoles of MDA per milligram of protein, using the molar extinction coefficient of the chromophore as  $1.56 \times 10^5 \text{ M}^{-1} \text{ cm}^{-1}$ .

**2.4.2.2. Measurement of SOD.** The method mentioned by Kono et al. (Kono, 1978) was utilized for assessment of SOD level in liver PMS. SOD level was highlighted in units of SOD per milligram of protein (SOD units/mg Pr).

**2.4.2.3. Estimation of GSH levels.** The technique highlighted by Jollow et al. (1974) was successfully utilized for estimation of GSH. The GSH level was estimated and represented as nmoles of GSH per  $\mu\text{g}$  of protein (nmoles of GSH/ $\mu\text{g}$  Pr).

**2.4.2.4. Estimation of proinflammatory cytokines, TNF- $\alpha$ .** An ELISA kit (RayBiotech, Inc) was used for measurement of TNF- $\alpha$  levels in prepared liver homogenates.

#### 2.5. Statistical analysis

The one-way analysis of variance (ANOVA), followed by the Tukey test was used for comparison of means of various treatments and statistical analysis of data. Differences between the means of all observations were considered statistically significant at  $p < 0.05$ . Experimental data expressed as mean  $\pm$  standard deviation (SD).

### 3. Results and discussion

#### 3.1. Synthesis and characterization of NODM

The reaction of unprotected hydroxyl groups of monosaccharides with long hydrocarbon chain amines in alcoholic medium has been

reported in scientific literature (Lockhoff and Stadler, 1998). In the present reaction, the unprotected hydroxyl group of mannose reacted with the amine group of stearylamine, resulted in the formation of a secondary amine bond between them. The obtained NODM was pale yellow crystals with the yield in the range of 78.61–84.13%. The physical characteristics like colour as well as solubility of both mannose and stearylamine were examined to preliminarily confirm product formation from the resulting reaction. The examined physical characteristics are highlighted in Table 1. D-mannose was a white, water soluble powder whereas the synthesized NODM was pale yellow crystals with solubility in organic solvent. There was change in the solubility pattern of mannose and NODM confirming the formation of a new reaction product.

##### 3.1.1. FTIR

FTIR spectra of D-Mannose, stearylamine, and synthesized NODM were recorded and shown in Fig. 1. In the spectrum of D-Mannose, broad peak at  $3398 \text{ cm}^{-1}$  and intense peak at  $2926 \text{ cm}^{-1}$  indicate the presence of  $-\text{OH}$  stretching and  $-\text{CH}_2$  stretching vibrations. Vibrational signals at  $1064$  and  $1638 \text{ cm}^{-1}$  indicate  $\text{C}=\text{O}$  stretching of either alcohol or aldehyde groups in mannose. In the spectrum of stearylamine, the sharp lower intensity peak at  $3331 \text{ cm}^{-1}$  indicate  $-\text{NH}_2$  stretching of primary amine group of stearylamine. Vibrational signals at  $2917$  and  $2849 \text{ cm}^{-1}$  indicate  $-\text{CH}_2$  stretching of the long alkyl chain. These two peaks were found to be more intense than that of mannose due to presence of long alkyl chain in stearylamine. Vibrational peaks at  $1606$  and  $1471 \text{ cm}^{-1}$  indicate presence of  $-\text{NH}_2$  and  $-\text{CH}_2$  bending. Spectrum of NODM showed lower intensity peak at  $3383 \text{ cm}^{-1}$ . This is due to the combination of  $-\text{NH}_2$  stretching of stearylamine and  $-\text{OH}$  stretching of mannose. Peak at  $1606 \text{ cm}^{-1}$  observed in stearylamine appears at lower intensity in NODM, indicating the conversion of primary amine (stearylamine) to secondary amine (NODM). Reduced intensity of peaks at  $1606 \text{ cm}^{-1}$  and  $3383 \text{ cm}^{-1}$  indicates the secondary amine linkage between mannose and stearylamine.

##### 3.1.2. Proton NMR

Proton NMR spectrum of the synthesized NODM is represented in Fig. 2. In the proton NMR spectrum, the presence of a lower intensity  $-\text{NH}$  proton signal at  $2.7 \text{ ppm}$  indicates the secondary amine linkage between mannose and stearylamine.

### 3.2. Preparation and characterization of curcumin loaded NLCs

NODM was incorporated into the NLCs by a melt homogenization ultrasonication technique. The solid lipid, liquid lipid and surfactant were selected for development of phytoactive loaded NLCs were selected based on their solubilization potential of curcumin. Numerous solid and liquid lipids were screened to understand the solubility of curcumin in lipids. Stearic acid and oleic acid showed maximum potential to solubilize curcumin thus, these lipids were selected for development of lipophilic matrix of NLCs. The surfactant was also selected based its solubilization potential of curcumin. To stabilize NLCs particles and minimize leaching loaded curcumin from lipid matrix of NLCs, the surfactant which showed least potential to solubilize curcumin was selected. Tween 20 showed least potential to solubilize curcumin thus, it was selected surfactant to stabilize curcumin loaded NLCs. The formulation variables like total lipid (% w/v), surfactant concentration (% w/v) and lipid: drug ratio were optimized previously using Box-Behnken study design by selecting particle size (nm) and zeta potential (mV) as responses.

NLCs with and without NODM were characterized for their size and entrapment efficiency. The conventional and mannosylated curcumin NLCs revealed particle sizes of 170.4 and 181 nm, respectively, as shown in Figs. 3 and 4. Particle size of the nanocarrier governs their uptake in hepatic parenchymal cells (Hashida et al., 1998; Liang et al., 2005). Numerous scientific experts have reported that nanocarriers with particle size less than 200 nm can efficiently engulf by hepatic parenchymal cells and generate significant biological effects. Both drug loaded NLCs revealed particle size less than 200 nm which confirmed its suitability for hepatic targeted drug delivery. The Entrapment efficiency of curcumin in conventional and mannosylated NLCs was found to be 83.41 and 80.19%.

NODM curcumin NLCs revealed lower zeta potential than conventional curcumin NLCs as represented in Table 2. The mannose conjugation on the surface of NLCs was confirmed by the zeta potential study. The decrease in the zeta potential value of curcumin loaded NLCs with increased concentration of NODM in NLCs from zero to 10% w/w of total lipids were the major findings of the present study. The reduction in the zeta potential from  $-12.19 \pm 0.41$  to  $-34.19 \pm 0.461$  mV for the conventional curcumin NLCs and the NODM conjugated curcumin NLCs at 10% NODM concentration respectively, could be attributed to the presence of mannose on the surface of NLCs as they contribute negative charge due to presence of ionizable hydroxy ( $\text{OH}^-$ ) group.

The decrease zeta potential of curcumin loaded NLCs with increased NODM concentration confirmed the presence of NODM on the surface of the NLCs as desired for the hepatocytes targeted delivery of curcumin. Thus, the zeta potential experiment was successfully utilized to validate the incorporation of NODM on curcumin NLCs surface.

### 3.3. Assessment of *in vivo* hepatoprotective potential

#### 3.3.1. Serum liver injury markers

The structural integrity damage of hepatocytes results in the release of AST and ALT enzymes in blood plasma. Thus, elevated levels of these enzymes in plasma indicate hepatocellular damage. Elevation of AST and ALT levels due to administration of  $\text{CCl}_4$  in experimental animals confirmed hepatic cellular damage (Sallie et al., 1991).  $\text{CCl}_4$  administration in experimental animals resulted in 2368.06% elevation in ALT level compared to group I (VC). The elevated level of serum liver injury marker like ALT was a sign of hepatotoxicity induction in rats. The four weeks treatment with conventional curcumin NLCs and mannosylated curcumin NLCs resulted a significant reduction in elevated ALT levels by  $52.73 \pm 2.981\%$  and  $63.17 \pm 3.472\%$  respectively as represented in Table 3. The standard hepatoprotective drug Liv-52 (Group III) administration to hepatotoxic rats resulted  $45.75 \pm 2.78\%$  reduction in ALT level. The formulated mannose functionalized curcumin NLCs dispersion was successful in a significant reduction ( $p < 0.05$ ) of elevated ALT levels

in experimental animals compared to conventional curcumin NLCs and Liv-52. This could be attributed due to enhanced accumulation of curcumin in hepatocytes. This *in vivo* liver protective study data supported the claim of hepatocyte targeting potential of synthesized targeting ligand.

Similarly, AST level was elevated by 980.73% due to administration of  $\text{CCl}_4$  compared to group I (VC). The conventional curcumin NLCs reduced elevated AST level by  $75.42 \pm 3.17\%$ . However, mannosylated curcumin NLCs revealed significantly better ( $p < 0.05$ ) reduction of elevated AST compared to conventional curcumin NLCs. This the hypothesis of hepatocyte targeting potential of NODM was confirmed on the basis of significantly better results with mannosylated curcumin NLCs.

#### 3.3.2. Antioxidant parameters

**3.3.2.1. LPO.** LPO measured as MDA content in liver PMS.  $\text{CCl}_4$  administration resulted in an elevation in MDA level by 443.39%. The four weeks treatment with mannosylated curcumin NLCs and conventional curcumin NLCs resulted in a reduction in MDA content by  $61.73 \pm 3.17\%$  and  $57.07 \pm 2.73\%$  respectively. The standard drug Liv-52 reduced the elevated MDA content by  $50.74 \pm 2.18\%$  on four week treatment. The curcumin loaded NLCs showed significantly better results ( $p < 0.05$ ) compared to standard drug (Fig. 5).

**3.3.2.2. SOD.** The positive control  $\text{CCl}_4$  group revealed a significantly low ( $p < 0.05$ ) SOD levels ( $0.504 \pm 0.089$  SOD units/mg Pr) compared to VC group. Treatment with standard drug Liv-52 for four weeks showed a 3 times increase ( $1.4903 \pm 0.1078$  SOD units/mg Pr) in SOD levels. The mannosylated curcumin NLCs treatment resulted in 7 times increase ( $3.2518 \pm 0.2365$  SOD units/mg Pr) in SOD level, whereas conventional curcumin NLCs treatment showed 5 times increase in SOD level ( $2.2122 \pm 0.3805$  SOD units/mg Pr) (Fig. 6). The mannosylated curcumin NLCs revealed significantly better ( $p < 0.05$ ) results than conventional curcumin NLCs with respect to the elevation of reduced SOD level. This could be attributed due to the better uptake of mannose anchored curcumin NLCs in hepatocytes than that of conventional curcumin NLCs. Thus mannose surface conjugation strategy could be viable and remarkable alternative for liver cell targeting of phytoactive loaded nanocarriers.

**3.3.2.3. GSH.** The total GSH level in PC group was significantly low ( $p < 0.05$ ) by  $\text{CCl}_4$  administration compared to VC group. The mannosylated curcumin NLCs successfully increased total GSH level by 8 times in four weeks treatment. The conventional curcumin NLCs showed comparable results with an increase in total GSH level by 6.96 times however it was found to be less effective compared to mannosylated curcumin NLCs (Fig. 7). The Tukey test showed a significant difference ( $p < 0.05$ ) between the results showed by mannosylated curcumin NLCs and conventional curcumin NLCs. The result of the study confirmed effectiveness of NODM for targeting of curcumin loaded NLCs to hepatocytes.

**3.3.2.4. Proinflammatory cytokine.** The administration of  $\text{CCl}_4$  resulted in a significant elevation of the proinflammatory cytokine  $\text{TNF-}\alpha$  level ( $610.18 \pm 9.146$  TNF Pg/ml) in PC group. The elevation of  $\text{TNF-}\alpha$  levels was an indication of hepatic injury induction. The four weeks treatment with mannosylated curcumin NLCs significantly reduced ( $p < 0.05$ ) the increased levels of  $\text{TNF-}\alpha$  ( $144.56 \pm 2.51$  TNF Pg/ml) compared to conventional curcumin NLCs ( $216.49 \pm 4.02$  TNF Pg/ml) (Fig. 8). Whereas, standard Liv-52 reduced an increased  $\text{TNF-}\alpha$  level up to  $152.62 \pm 4.95$  TNF Pg/ml. The results obtained with mannose anchored curcumin loaded NLCs were significantly better than both conventional NLCs as well as Liv-52 which confirm the targeting potential of the synthesized ligand.

#### 4. Conclusion

In the current investigation, an attempt has been made to synthesize novel hepatocytes targeting ligand i.e., NODM for efficient delivery of curcumin encapsulated NLCs. FTIR and <sup>1</sup>H NMR techniques confirmed the correctness of the adopted synthetic procedure. Melt homogenization ultrasonication technique was found to be an effective method for the fabrication of curcumin loaded NLCs. The selected method was found to be suitable for the generation of NLCs with better particle size and curcumin entrapment efficiency. The particle diameter of NLCs less than 200 nm confirmed its suitability for hepatocyte targeted drug delivery. *In vivo* hepatoprotective potential studied in CCl<sub>4</sub> induced liver injury animal model confirmed hepatocytes targeting potential of synthesized NODM by effectively reducing serum liver injury markers and proinflammatory cytokines compared to conventional NLCs. However, additional *in vivo* pharmacokinetic studies and organ distribution studies are required for exact confirmation of the targeting potential of the synthesized ligand. Thus, the synthesized mannose anchored stearylamine i.e., NODM could be a viable alternative for hepatocyte targeting of nanomedicines.

#### Authorship statement

All persons who meet authorship criteria are listed as authors, and all authors certify that they have participated sufficiently in the work to take public responsibility for the content, including participation in the concept, design, analysis, writing, or revision of the manuscript. Furthermore, each author certifies that this material or similar material has not been and will not be submitted to or published in any other publication before its appearance in Current Research in Pharmacology and Drug Discovery.

#### CRediT authorship contribution statement

**Manish Kumar Gupta:** Conceptualization, Methodology, Formal analysis, Data curation, Writing – original draft, Writing – review & editing, Visualization. **Vipul Sansare:** Conceptualization, Investigation, Resources, Writing – review & editing, Supervision. **Birendra Shrivastava:** Conceptualization, Methodology, Writing – review & editing, Supervision. **Santosh Jadhav:** Conceptualization, Methodology, Investigation, Resources, Writing – review & editing. **Prashant Gurav:** Conceptualization, Methodology, Investigation, Resources, Writing – review & editing.

#### Declaration of competing interest

The authors declare that they have no competing interests.

#### Acknowledgements

Authors would like to say thanks to Department of Pharmaceutics, Bombay College of Pharmacy (Mumbai, India) and Department of Pharmacology, Indira Institute of Pharmacy (Sadavali, India) for technical support. We are thankful to Dr. Lebogang Katata-Seru, North-West University, Mahikeng, South Africa for excellent technical advice.

#### References

Bartneck, M., Warzecha, K.T., Tacke, F., 2014. Therapeutic targeting of liver inflammation and fibrosis by nanomedicine. *Hepatobiliary Surg. Nutr.* 3, 364–376. <https://doi.org/10.3978/j.issn.2304-3881.2014.11.02>.

Bei, Y., Yuan, Z., Zhang, L., 2014. Novel self-assembled micelles based on palmitoyl-trimethyl-chitosan for efficient delivery of harmine to liver cancer. *Exp. Opin. Drug Deliv.* 11, 843–854.

Bonferoni, M.C., Rossi, S., Cornaglia, A.I., Mannucci, B., Grisoli, P., Vigani, B., 2018. Essential oil-loaded lipid nanoparticles for wound healing. *Int. J. Nanomed.* 13, 175–186. <https://doi.org/10.2147/IJN.S152529>.

Castangia, I., Caddeo, C., Manca, M.L., Casu, L., Latorre, A.C., Díez-Sales, O., Ruiz-Sauri, A., Bacchetta, G., Fadda, A.M., Manconi, M., 2015. Delivery of liquorice extract by liposomes and hyalurosomes to protect the skin against oxidative stress injuries. *Carbohydr. Polym.* 134, 657–663. <https://doi.org/10.1016/j.carbpol.2015.08.037>.

Craparo, E., Sardo, C., Serio, R., 2014. Galactosylated polymeric carriers for liver targeting of sorafenib. *Int. J. Pharm.* 466, 172–180.

Farzaei, M.H., Zobeiri, M., Parvizi, F., El-senduny, F.F., Marmouzi, I., Coy-barrera, E., Naseri, R., Nabavi, S.M., Rahimi, R., Abdollahi, M., 2018. Curcumin in liver diseases: a systematic review of the cellular mechanisms of oxidative stress and clinical perspective. *Nutrients* 10, 855. <https://doi.org/10.3390/nu10070855>.

Guhagarkar, S.A., Shah, D., Patel, M.D., Sathaye, S.S., Devarajan, P.V., 2015. Polyethylene sebacate-silymarin nanoparticles with enhanced hepatoprotective activity. *J. Nanosci. Nanotechnol.* 15, 4090–4093. <https://doi.org/10.1166/jnn.2015.9518>.

Guo, H., Zhang, D., Li, T., 2014. *In vitro* and *in vivo* study of gal-os self-assembled nanoparticles for liver-targeting delivery of doxorubicin. *J. Pharm. Sci.* 103, 987–993.

Hashida, M., Takemura, S., Nishikawa, M., Takakura, Y., 1998. Targeted delivery of plasmid DNA complexed with galactosylated poly(L-lysine). *J. Contr. Release* 53, 301–310.

Irache, J.M., Salman, H.H., Gamazo, C., Espuelas, S., 2008. Mannose-targeted systems for the delivery of therapeutics. *Expert Opin* 5, 703–724. <https://doi.org/10.1517/17425240802168025>.

Jain, K., Kesharwani, P., Gupta, U., Jain, N.K., 2012. A review of glycosylated carriers for drug delivery. *Biomaterials* 33, 4166–4186. <https://doi.org/10.1016/j.biomaterials.2012.02.033>.

Jollow, D., Mitchell, L., Zampaglione, N., Gillette, J., 1974. Bromobenzene induced liver necrosis: protective role of glutathione and evidence for 3,4-bromobenzenoxide as the hepatotoxic intermediate. *Pharmacology* 11, 151–169.

Kakkar, V., Kaur, I.P., 2012. Preparation, characterization and scale-up of sesamol loaded solid lipid nanoparticles. *Nanotechnol. Dev.* 2, 40–45. <https://doi.org/10.4081/nd.2012.e8>.

Kono, Y., 1978. Generation of superoxide radical during autooxidation of hydroxylamine and an assay for superoxide dismutase. *Arch. Biochem. Biophys.* 186, 189–195.

Liang, H., Yang, T., Huang, C., Chen, M., Sung, H., 2005. Preparation of nanoparticles composed of poly(gamma-glutamic acid)-poly (lactide) block copolymers and evaluation of their uptake by HepG2 cells. *J. Contr. Release* 105, 213–225.

Lockhoff, O., Stadler, P., 1998. Syntheses of glycosylamides as glycolipid analogs. *Carbohydr. Res.* 314, 13–24.

Mayuren, C., Reddy, V.V., Priya, S.V., 2010. Protective effect of Livactine against CCl<sub>4</sub> and paracetamol induced hepatotoxicity in adult Wistar rats. *N. Am. J. Med. Sci.* 2, 491–495. <https://doi.org/10.4297/najms.2010.2491>.

Mimche, P.N., Taramelli, D., Vivas, L., 2011. The plant-based immunomodulator curcumin as a potential candidate for the development of an adjunctive therapy for cerebral malaria. *Malar. J.* 10, 1–9. <http://www.malariajournal.com/content/10/S1/S10>.

Mohanalakshmi, S., Palei, N., Kumar, A., Babu, R., 2019. Solid lipid nanoparticles of Annona muricata fruit extract: formulation, optimization and *in vitro* Cytotoxicity studies. *Drug Dev. Ind. Pharm.* 45, 577–586. <https://doi.org/10.1080/03639045.2019.1569027>.

Nahr, F.K., Ghanbarzadeh, B., Kafil, H.S., Hoseini, M., 2019. The colloidal and release properties of cardamom oil encapsulated nanostructured lipid carrier. *J. Dispersion Sci. Technol.* 42. <https://doi.org/10.1080/01932691.2019.1658597>.

Permana, A.D., Utami, R.N., Courtenay, A.J., Manggau, M.A., Donnelly, R.F., Rahman, L., 2020. Phytosomal nanocarriers as platforms for improved delivery of natural antioxidant and photoprotective compounds in propolis: an approach for enhanced both dissolution behaviour in biorelevant media and skin retention profiles. *J. Photochem. Photobiol. B Biol.* 205, 111846. <https://doi.org/10.1016/j.jphotobiol.2020.111846>.

Pranatharthi, S., Patel, M.D., Malshe, V.C., Gorakshakar, A., Madkai, K., Ghosh, K., Padma, V., Pranatharthi, S., Patel, M.D., Malshe, V.C., Dujori, V., Gorakshakar, A., 2017. Asialoglycoprotein receptor targeted delivery of doxorubicin nanoparticles for hepatocellular carcinoma. *Drug Deliv.* 24, 20–29. <https://doi.org/10.1080/10717544.2016.1225856>.

Prathyusha, M., Manjunath, K., Tippanna, S., Shivanandappa, B., 2014. Bixin loaded solid lipid nanoparticles for enhanced hepatoprotection – preparation, characterisation and *in vivo* evaluation. *Int. J. Pharm.* 473, 485–492. <https://doi.org/10.1016/j.ijpharm.2014.07.027>.

Raposo, D., Costa, R., Petrova, K.T., Brito, C., Scotti, M.T., Cardoso, M.M., 2020. Development of novel galactosylated PLGA nanoparticles for hepatocyte targeting using molecular modelling. *Polymers* 12, 1–18. <https://doi.org/10.3390/polym12010094>.

Rechnagel, R., Eaj, G., 1973. Carbon tetrachloride hepatotoxicity: an example of lethal cleavage. *CRC Crit. Rev. Toxicol.* 2, 263–297.

Rivera-espinoza, Y., Muriel, P., 2009. Pharmacological actions of curcumin in liver diseases or damage. *Liver Int.* 1457–1466. <https://doi.org/10.1111/j.1478-3231.2009.02086.x>.

Sallie, R., Tredger, J., Williams, R., 1991. Drugs and the liver part 1: testing liver function. *Biopharm Drug Dispos.* 12, 251–259.

Sansare, V., Patel, N., Patankar, N., 2019. Design, optimization and characterization of lamivudine loaded solid lipid nanoparticles for targeted delivery to brain. *Int. Res. J. Pharm.* 10, 143–148. <https://doi.org/10.7897/2230-8407.100258>.

Sansare, V., Warriar, D., Shinde, U., 2020. Cellular trafficking of nanocarriers in alveolar macrophages for effective management of pulmonary tuberculosis. *J. Tuberc.* 3, 1016.

Shah, S.M., Pathak, P.O., Jain, A.S., Barhate, C.R., Nagarsenker, M.S., 2013. Synthesis, characterization, and *in vitro* evaluation of palmitoylated arabinogalactan with

- potential for liver targeting. *Carbohydr. Res.* 367, 41–47. <https://doi.org/10.1016/j.carres.2012.11.025>.
- Singh, N., Khullar, N., Kakkar, V., Kaur, I.P., 2015. Sesamol loaded solid lipid nanoparticles : a promising intervention for control of carbon tetrachloride induced hepatotoxicity. *BMC Compl. Alternative Med.* 15, 142. <https://doi.org/10.1186/s12906-015-0655-y>.
- Tang, J., Ge, Y., 2017. Development and evaluation of novel Eucalyptus essential oil liposomes/chitosan composite sponges for medical use. *Fibers Polym.* 18, 424–433. <https://doi.org/10.1007/s12221-017-6983-4>.
- Tung, B.T., Hai, N.T., Son, P.K., 2011. Hepatoprotective effect of Phytosome Curcumin against paracetamol-induced liver toxicity in mice. *Brazilian J. Pharm. Sci.* 53, 1–13.
- Vasanthkumar, T., Hanumanthappa, M., Bt, P., Hanumanthappa, S.K., Hanuman, M., Hanu, S.K., 2017. Hepatoprotective effect of curcumin and capsaicin against lipopolysaccharide induced liver damage in mice. *Pharmacogn. J.* 9, 947–951. <https://doi.org/10.5530/pj.2017.6.148>.
- Wills, E., 1966. Mechanisms of lipid peroxide formation in animal tissue. *Biochem. J.* 99, 667–676.
- Witoonsaridsilp, W., Paeratakul, O., Panyarachun, B., Sarisuta, N., 2012. Development of mannoseylated liposomes using synthesized N -octadecyl- D - mannopyranosylamine to enhance gastrointestinal permeability for protein delivery. *AAPS PharmSciTech* 13, 699–706. <https://doi.org/10.1208/s12249-012-9788-1>.
- Wu, D-Q, 2009. Galactosylated fluorescent labeled micelles as a liver targeting drug carrier. *Biomaterials* 30, 1363–1371.